SUPPLEMENTAL MATERIALS

ASCE *Journal of Geotechnical and Geoenvironmental Engineering*

Theoretical *t-z* Curves for Axially Loaded Piles

Abigail H. Bateman, Jamie J. Crispin, Paul J. Vardanega, and George E. Mylonakis

DOI: 10.1061/(ASCE)GT.1943-5606.0002753

www.ascelibrary.org

Fitting of soil constitutive models

The fitting of the model parameters from the eight simplified soil constitutive models, summarised in Table 1, to two representative soil samples, is discussed in more detail in this supplement. The results of the fitting analysis are provided in the main paper. The method presented requires an experimental stress-strain curve, e.g., from a triaxial test, making it easily applicable to any problem where soil stress-strain data is available. The analysis in this work aims to provide an example of the method presented in the main text, not site-specific design values. From the two illustrative examples discussed in the main text, two soil samples: (A) a high plasticity Pisa clay and, (B) a flocculated kaolinite, are selected to represent the material at the mid-depth of each example pile using digitised soil test data from Soga (1994).

First, a test on an undisturbed sample of a high plasticity Pisa clay was selected, obtained from a depth of 10m, and is described as a "dark grey high plastic clay" (Soga (1994)). This sample was reported to have a plasticity index of 48.4%, an OCR of 1.5 and was isotopically consolidated at a mean pressure of 85 kPa (with an estimated effective vertical stress of 109 kPa, Soga (1994)). To investigate the anisotropic properties of the Pisa clay, Soga (1994) used both horizontally and vertically cut samples as well as both isotopically and anisotropically consolidated samples. Vertically cut samples are selected for the fitting analysis as they are expected to best represent the soil response from an axially loaded pile.

Second, a test on a remoulded flocculated kaolinite sample reported in Soga (1994) was selected. The sample preparation resulted in a material with a high initial void ratio, rigid soil fabric and a plasticity index of 29%. These samples were then isotopically consolidated to 98 kPa (OCR = 1), selected since this best represented the stress state of soil at approximately 5 m depth (above the water table).

To obtain the stress-strain (τ-γ) response of the two materials, Soga (1994) performed undrained triaxial compression testing on each sample. The tests were conducted at three axial strain rates (0.5%, 0.05%, and 0.005% per minute) for the kaolinite sample and at a single strain rate (0.5% per minute) for the Pisa clay. The strain rate had limited effect on the undrained strength and shape of the stress-strain curve of the flocculated kaolinite (Soga (1994)). Therefore, the test conducted at 0.5% per minute was selected because tests at this strain rate are available for both materials. In addition, isotopically consolidated samples were selected, as this is a required assumption to fit the simplified soil constitutive models presented here. From the test results (τ-γ), the undrained shear strength, c_u, for both materials can be interpreted as the maximum shear stress reached (45 kPa for Pisa clay and 29 kPa for kaolinite, see Fig. 6(a) and 6(b), respectively, in the main text).

Additionally, Soga (1994) conducted torsional cyclic shear tests on the same samples to investigate stiffness degradation. The results of which are used to determine the G_{max} of each soil (29 MPa for Pisa clay and 78 MPa for kaolinite, Soga (1994)) which provides the option of using the measured G_{max} instead of fitting the G_i in each model (alternative soil testing is available, e.g., seismic CPT). The kaolinite soil samples were tested at two frequencies (0.1 Hz and 0.5 Hz) which was acknowledged to significantly affect the G_{max}. Samples tested at a frequency of 0.5 Hz were selected because such results are available for both materials. If the small strain region is unlikely to be important for the problem under consideration, a measured G_{max} is not required as this value can be fit as a model parameter, G_i. Full details of both materials and subsequent soil testing can be found in Soga (1994).

The eight soil constitutive models summarised in Table 1 are fitted to digitised data points along the selected isotropic undrained triaxial test results (at 0.5% per minute) using a non-linear least-squares fitting. The results of the fitting for each soil constitutive model, using various assumptions (discussed below), are shown in Figs. S1-S8, with the respective parameters given in Tables S1-S8.

As multiple fittings for each soil constitutive model are considered, a method to select the most appropriate fitted line is required. To assess each fitting, the measured shear stress from the triaxial test data can be compared to that predicted by each model and an error bound obtained, based on a selected proportion of the data (95% is used here). The fitting with the smallest error bound is selected (or an alternative method can be applied). The error bounds for each fitting are provided in Tables S1-S8. As discussed in the main paper this method does not bias the result towards conservative predictions.

In some cases, model parameters can be directly interpreted from the test results instead of being employed as a fitting parameter. From the models considered, it is possible to interpret two model parameters as soil parameters: (1) $\tau_{max} = c_u$ interpreted from the undrained triaxial test data, (2) $G_i = G_{max}$ interpreted from the torsional cyclic shear results. It is also possible to interpret γ_{50} from the triaxial test results, but this has not been attempted here due to its reliance on an interpreted c_u and the effect scatter of the data can have on this value. Different combinations of fitted (i.e., G_i and/or τ_{max} as free parameters) and interpreted (i.e., $G_i = G_{max}$ and/or $\tau_{max} = c_u$) parameters were considered. However, as can be seen from the τ-γ plots (Figs. S1-S8), reasonable results are not always obtained when τ_{max} is fitted (instead of using $\tau_{max} = c_u$). It was therefore decided to only consider $\tau_{max} = c_u$.

Data points within two stress ranges were considered for fitting: (1) all data points until failure ($0 \leq \tau \leq c_u$) and, (2) within a specified moderate stress range ($0.2\, c_u \leq \tau \leq 0.8\, c_u$). A better fit is obtained in the moderate stress range because this region limits the effect of scatter at the onset of plastic behaviour at the expense of accurately modelling small strain response (this approach was also employed in Vardanega and Bolton (2011)). Also, as the error bounds are calculated relative to the stress range of fitting, they are not directly comparable but give an idea of the respective fittings. To select the best constitutive model for the examples, it was decided to select the stress range ($0.2\, c_u \leq \tau \leq 0.8\, c_u$) as the 'desired' stress range for the two examples presented in the main paper.

When the results of each model are considered, some discussion points are noted. First, the linear constitutive model (Fig. S1 and Table S1) has high error bounds across the stress ranges considered. However, if the loading is not expected to exceed the small strain region, the model (with $G = G_{max}$) may provide a suitable estimate (Leung *et al*. 2010). Alternatively, the bi-linear model (Fig. S2 and Table S2) reduces the error bounds considerably, although higher errors are seen near the change in stiffness, τ_1. This model has the additional disadvantage that the fitted parameters have a limited physical interpretation.

Both the power law (Fig. S3 and Table S3) and the linear-power law (Fig. S4 and Table S4) models provide an excellent fit to the experimental results for the high plasticity Pisa clay, giving the exact same results in the stress range $0.2\, c_u \leq \tau \leq 0.8\, c_u$ (where the initial stiffness has no effect; for the examples presented in this work). Thus, when the small strain region is deemed important, the linear-power law model should be selected with a measured G_{max}, else the simpler power law model would be more suitable. The linear-power law model, with a fitted G_i, does not fit well over the stress range $0.2\, c_u \leq \tau \leq 0.8\, c_u$ as few data points are available to determine an initial stiffness. Additionally, in general the Ramberg-Osgood model (Fig. S5 and Table S5) can be seen to provide the best fit for both soil examples. This comes at a price as the model requires 3 deformation parameters.

The hyperbolic model (Fig. S6 and Table S6) provides a good fit for the kaolinite across the desired stress range. Due to the fitting parameter, R_f, which acts as a factor on the τ_{max}, this model does not perform well outside the specific stress range. Alternatively, the modified hyperbolic model (Fig. S7 and Table S7) provides a reasonable fit over the entire range and has the benefit of being able to incorporate a measured G_{max} with low error. It should be noted that when a fitted G_i is used in this model, large initial stiffness values are obtained (even though a reasonable overall fit is seen). Thus, the selected G_i has been limited to the measured value ($G_i = G_{max}$).

Finally, a similar result to the hyperbolic model, but with higher error bounds, is obtained from the exponential model (Fig. S8 and Table S8) due to the same R_f value. The selected fit for each soil constitutive model is shown in Fig. 6 of the main text.

Table S1: Parameters from the fitting of the linear model and the respective error bounds. c_u and G_{max} are interpreted values from Soga (1994).

Soil	Range	Parameters		Errors bounds for 95% of data (%)
		G (kPa)	τ_{max} (kPa)	
Pisa	$0 - c_u$	2,513	40.5	1314
		2,129	c_u	1569
		G_{max}	32.9	167
		G_{max}	c_u	226
	$0.2c_u - 0.8c_u$	3,468	29.8	144
		2,071	c_u	308
		G_{max}	23.0	113
		G_{max}	c_u	244
Kaolinite	$0 - c_u$	7,296	24.6	89
		6,451	c_u	113
		G_{max}	21.9	430
		G_{max}	c_u	456
	$0.2c_u - 0.8c_u$	9,266	19.5	47
		6,385	c_u	114
		G_{max}	15.6	124
		G_{max}	c_u	312

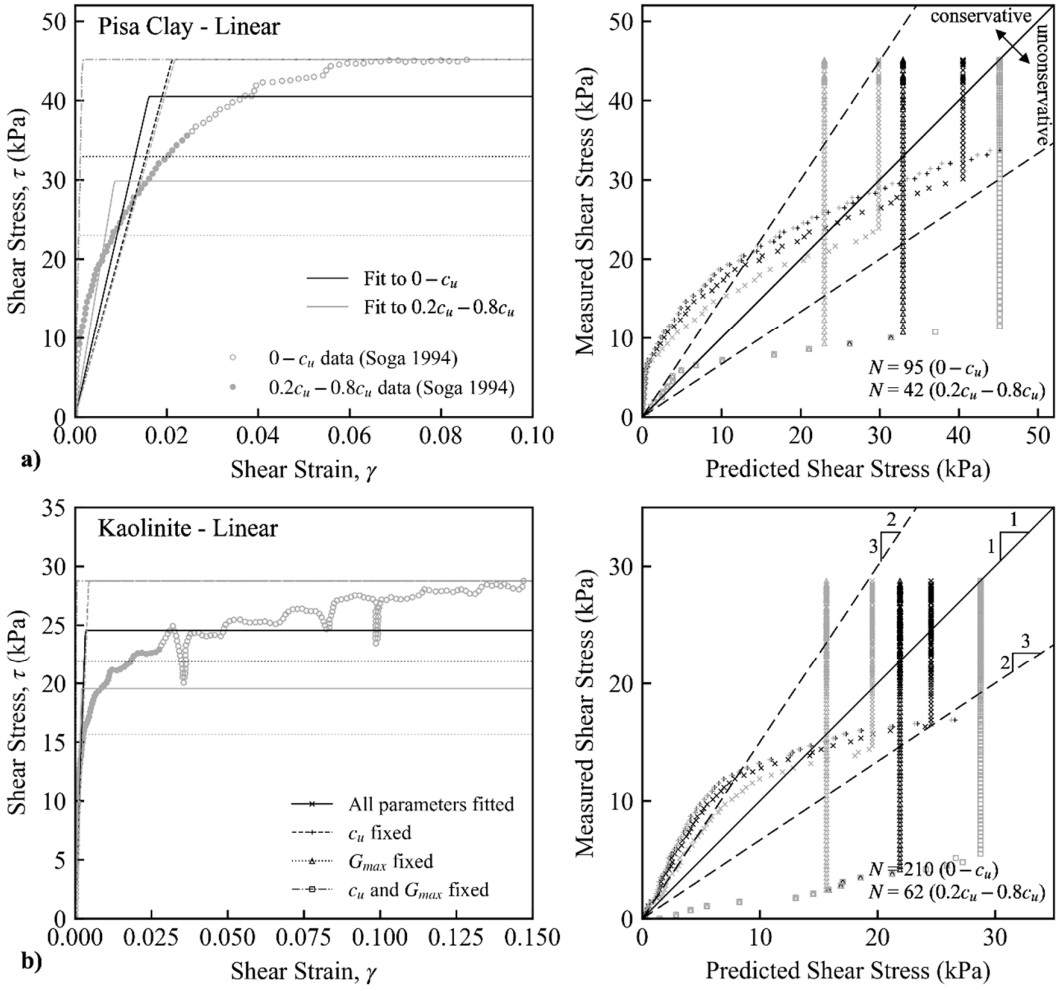

Figure S1: Fitting of the linear model to triaxial data in a) Pisa clay and b) kaolinite. Percentages in parentheses indicate the error bounds. ± 50% prediction bounds are provided for comparison. *N* denotes the number of data points considered in each range. (Data from Soga 1994.)

Table S2: Parameters from the fitting of the bi-linear model and the respective error bounds. c_u and G_{max} are interpreted values from Soga (1994).

Soil	Range	Parameters				Errors bounds for 95% of data (%)
		τ_{max} (kPa)	G_1 (kPa)	G_2 (kPa)	τ_1	
Pisa	$0 - c_u$	43.1	27,400	1,010	13.0	35.6
		c_u	27,400	930	13.6	40.5
		43.1	G_{max}	1,010	13.0	35.8
		c_u	G_{max}	930	13.6	39.8
	$0.2c_u - 0.8c_u$	33.2	19,500	1,320	11.8	18.0
		c_u	96,500	1,070	12.6	28.0
		33.8	G_{max}	1,260	11.8	20.0
		c_u	G_{max}	1,070	12.9	28.0
Kaolinite	$0 - c_u$	25.5	12,300	440	15.1	19.9
		c_u	11,200	110	18.5	28.3
		25.0	G_{max}	2,370	6.5	97
		c_u	G_{max}	1,310	8.0	135
	$0.2c_u - 0.8c_u$	21.5	12,800	1,190	12.8	9.6
		c_u	12,200	380	15.4	17.5
		21.3	G_{max}	2,050	8.6	34.6
		c_u	G_{max}	580	11.7	71

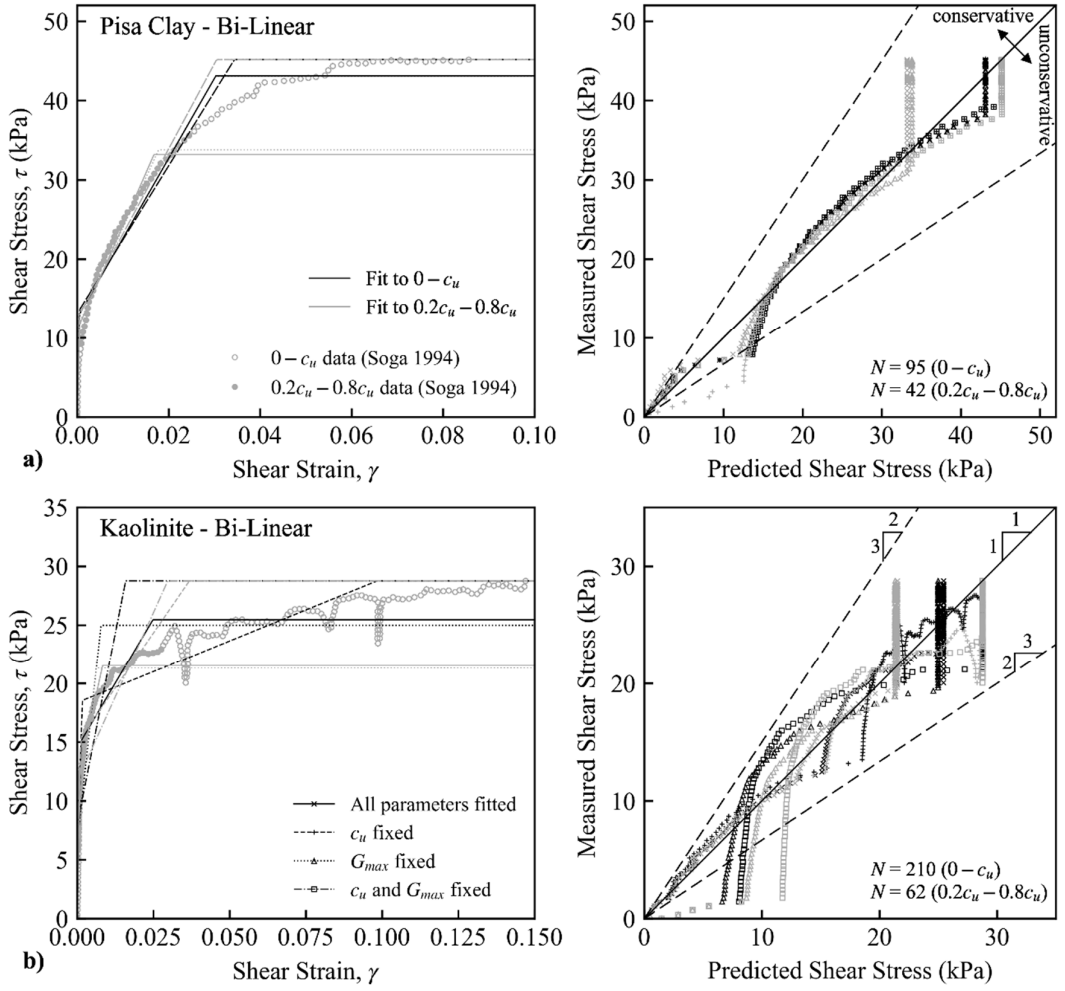

Figure S2: Fitting of the bi-linear model to triaxial data in a) Pisa clay and b) kaolinite. Percentages in parentheses indicate the error bounds. ± 50% prediction bounds are provided for comparison. *N* denotes the number of data points considered in each range. (Data from Soga 1994.)

Table S3: Parameters from the fitting of the power law model and the respective error bounds. c_u and G_{max} are interpreted values from Soga (1994).

Soil	Range	Parameters			Errors bounds for 95% of data (%)
		τ_{max} (kPa)	γ_{50}	b	
Pisa	$0 - c_u$	102.3	0.0910	0.33	65
		c_u	0.0079	0.38	25.6
	$0.2c_u - 0.8c_u$	57.4	0.0142	0.41	2.6
		c_u	0.0079	0.41	2.6
Kaolinite	$0 - c_u$	63.0	0.2031	0.20	134
		c_u	0.0040	0.20	131
	$0.2c_u - 0.8c_u$	52.2	0.0333	0.24	35.9
		c_u	0.0028	0.24	35.9

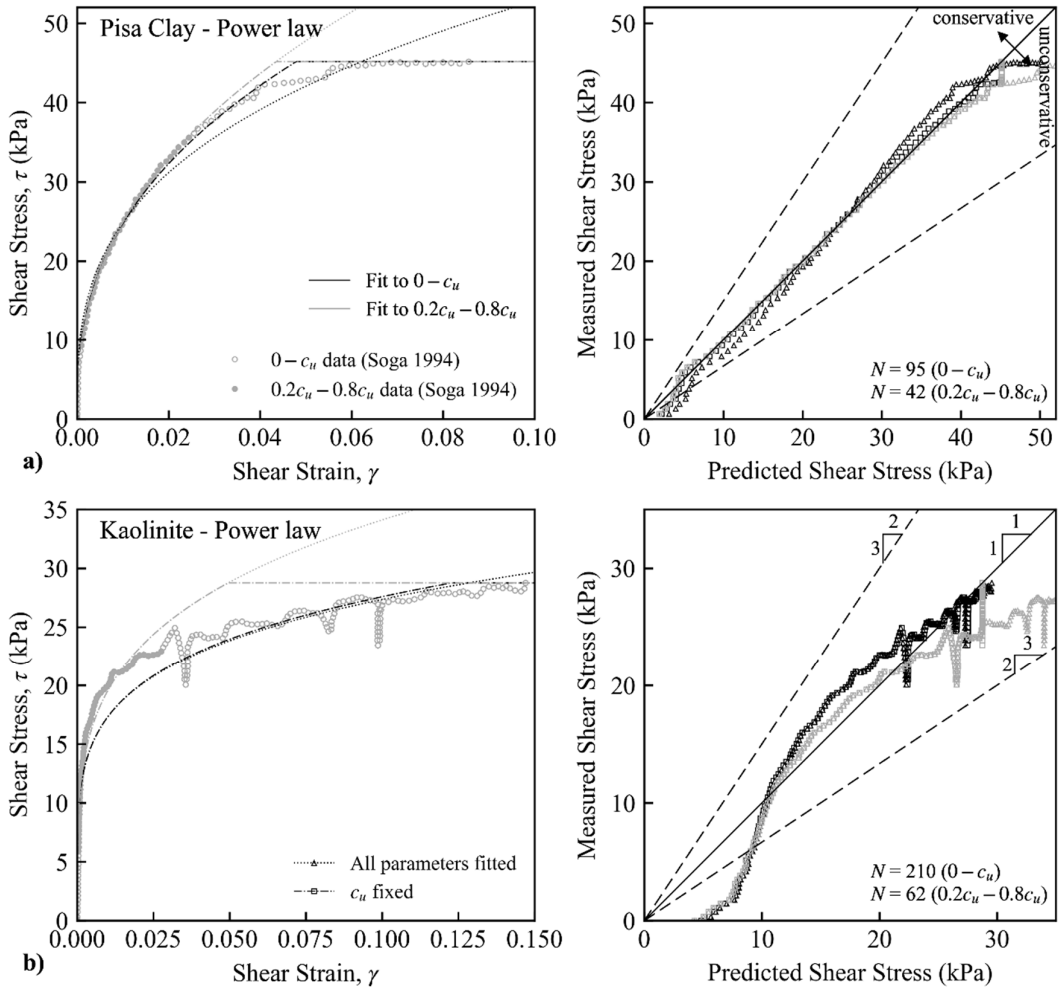

Figure S3: Fitting of the power law model to triaxial data in a) Pisa clay and b) kaolinite. Percentages in parentheses indicate the error bounds. ± 50% prediction bounds are provided for comparison. *N* denotes the number of data points considered in each range. (Data from Soga 1994.)

Table S4: Parameters from the fitting of the linear-power law model and the respective error bounds. c_u and G_{max} are interpreted values from Soga (1994).

Soil	Range	Parameters				Errors bounds for 95% of data (%)
		τ_{max} (kPa)	G_i (kPa)	γ_{50}	b	
Pisa	$0 - c_u$	75.3	35,400	0.0356	0.32	20.7
		c_u	35,700	0.0078	0.38	7.1
		54.2	G_{max}	0.0127	0.32	24.8
		c_u	G_{max}	0.0078	0.38	22.5
	$0.2c_u - 0.8c_u$	-	G_i	-	-	-
		-	G_i	-	-	-
		61.3	G_{max}	0.0167	0.41	2.6
		c_u	G_{max}	0.0079	0.41	2.6
Kaolinite	$0 - c_u$	39.2	12,600	0.0113	0.14	14.7
		c_u	12,600	0.0013	0.14	14.7
		39.3	G_{max}	0.0184	0.19	142
		c_u	G_{max}	0.0037	0.20	140
	$0.2c_u - 0.8c_u$	-	G_i	-	-	-
		-	G_i	-	-	-
		53.1	G_{max}	0.0355	0.24	35.9
		c_u	G_{max}	0.0028	0.24	35.9

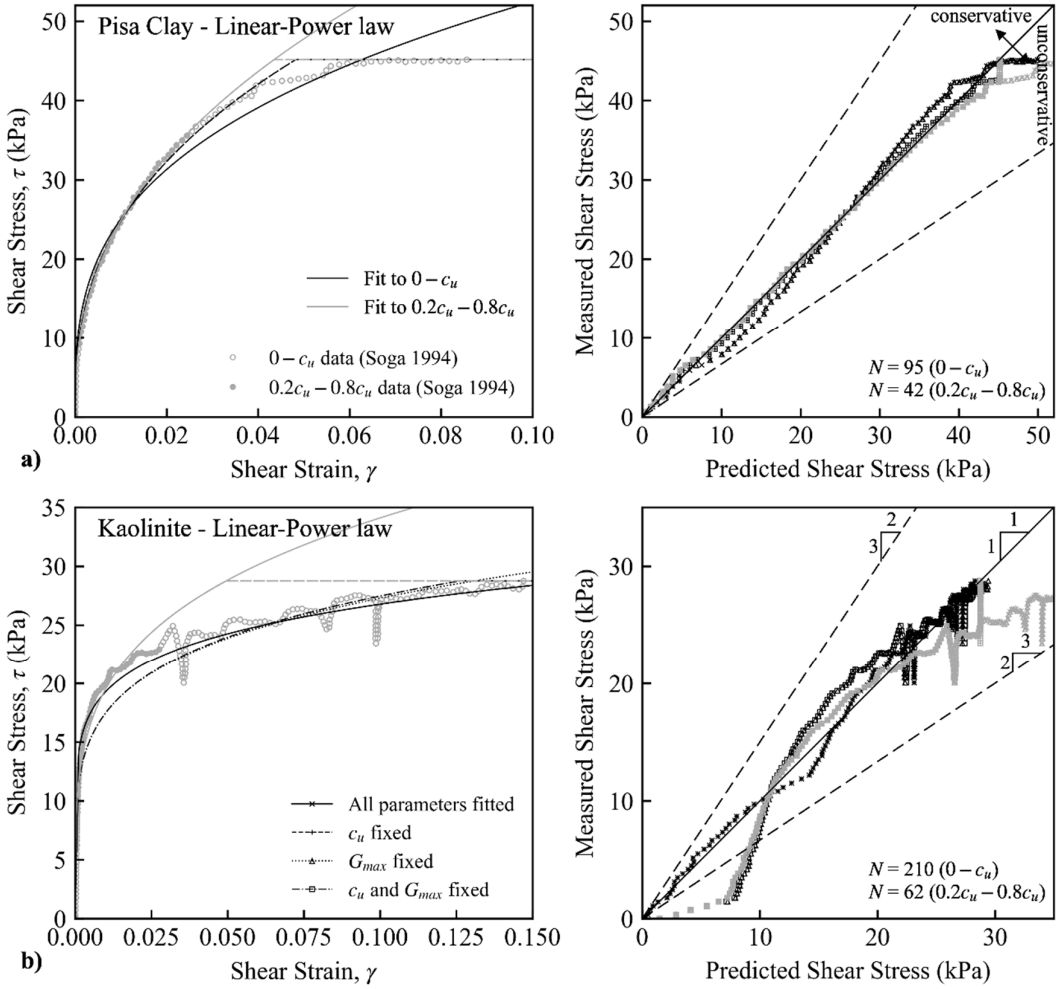

Figure S4: Fitting of the linear-power law model to triaxial data in a) Pisa clay and b) kaolinite. Percentages in parentheses indicate the error bounds. ± 50% prediction bounds are provided for comparison. *N* denotes the number of data points considered in each range. (Data from Soga 1994.)

Table S5: Parameters from the fitting of the Ramberg-Osgood model and the respective error bounds. c_u and G_{max} are interpreted values from Soga (1994).

Soil	Range	Parameters				Errors bounds for 95% of data (%)
		τ_{max} (kPa)	γ_r	c_1	c_2	
Pisa	$0 - c_u$	44.4	0.00063	4.91	2.69	26.1
		c_u	0.00069	4.80	2.71	24.4
	$0.2c_u - 0.8c_u$	35.6	0.00038	5.15	2.52	2.3
		c_u	0.00053	5.72	2.53	2.3
Kaolinite	$0 - c_u$	30.1	0.00223	1.82	7.90	12.1
		c_u	0.00214	1.75	7.90	12.1
	$0.2c_u - 0.8c_u$	22.7	0.00162	1.46	6.59	2.1
		c_u	0.00207	1.77	6.83	2.6

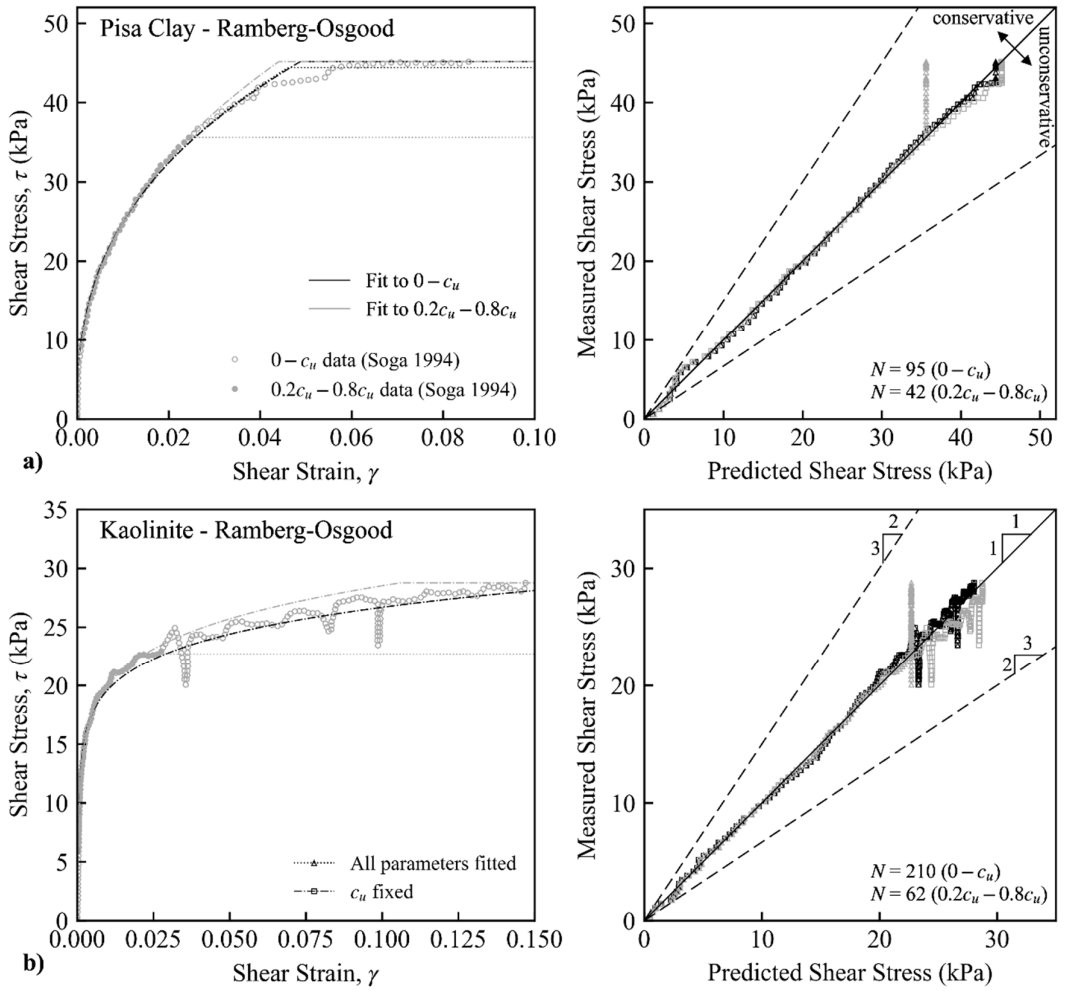

Figure S5: Fitting of the Ramberg-Osgood model to triaxial data in a) Pisa clay and b) kaolinite. Percentages in parentheses indicate the error bounds. ± 50% prediction bounds are provided for comparison. *N* denotes the number of data points considered in each range. (Data from Soga 1994.)

Table S6: Parameters from the fitting of the hyperbolic model and the respective error bounds. c_u and G_{max} are interpreted values from Soga (1994).

Soil	Range	Parameters			Errors bounds for 95% of data (%)
		τ_{max} (kPa)	G_i (kPa)	R_f	
Pisa	$0 - c_u$	c_u	5,730	0.91	528
		c_u	7,220	1	400
		c_u	G_{max}	1.19	74
		c_u	G_{max}	1	94
	$0.2c_u - 0.8c_u$	c_u	7,650	1.12	37.4
		c_u	6,340	1	57
		c_u	G_{max}	1.59	48.8
		c_u	G_{max}	1	98
Kaolinite	$0 - c_u$	c_u	14,940	1.11	21.7
		c_u	9,400	1	70
		c_u	G_{max}	1.20	198
		c_u	G_{max}	1	222
	$0.2c_u - 0.8c_u$	c_u	20,040	1.26	6.8
		c_u	12,110	1	40.1
		c_u	G_{max}	1.56	81
		c_u	G_{max}	1	140

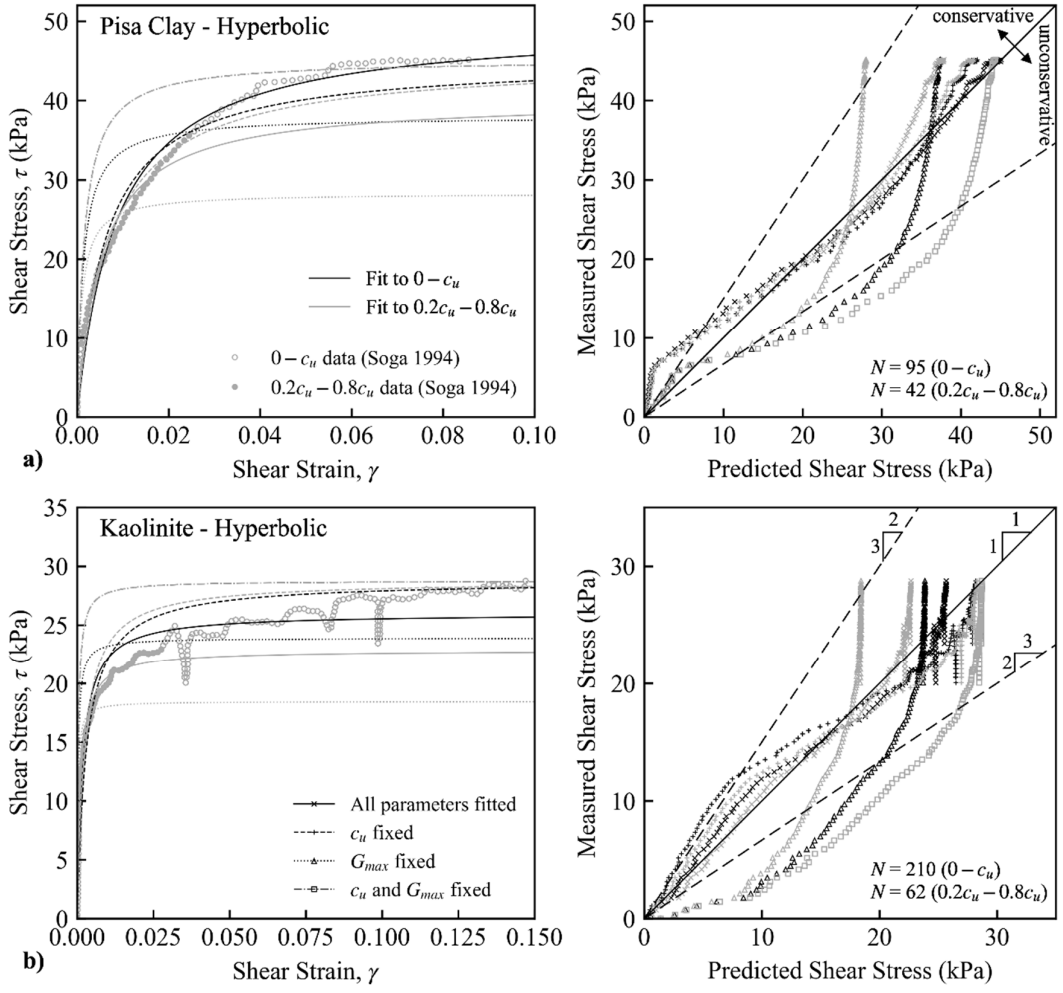

Figure S6: Fitting of the hyperbolic model to triaxial data in a) Pisa clay and b) kaolinite. Percentages in parentheses indicate the error bounds. ± 50% prediction bounds are provided for comparison. *N* denotes the number of data points considered in each range. (Data from Soga 1994.)

Table S7: Parameters from the fitting of the modified hyperbolic model and the respective error bounds. c_u and G_{max} are interpreted values from Soga (1994).

Soil	Range	Parameters				Errors bounds for 95% of data (%)
		τ_{max} (kPa)	G_i (kPa)	R_f	c_3	
Pisa	$0 - c_u$	c_u	45,980,000	0.84	0.00008	162
		c_u	9758	1	0.69	290
		c_u	G_{max}	0.85	0.13	205
		c_u	G_{max}	1	0.21	140
	$0.2c_u - 0.8c_u$	c_u	32,550,000	0.95	0.00013	19.9
		c_u	22,230,000	1	0.00021	15.9
		c_u	G_{max}	0.98	0.16	23.2
		c_u	G_{max}	1	0.17	21.7
Kaolinite	$0 - c_u$	c_u	47,850,000	1.08	0.00019	23.0
		c_u	70,590,000	1	0.00009	43.2
		c_u	G_{max}	1.09	0.13	20.8
		c_u	G_{max}	1	0.08	46.5
	$0.2c_u - 0.8c_u$	c_u	336,000	1.21	0.04	10.0
		c_u	101,750,000	1	0.00008	22.0
		c_u	G_{max}	1.21	0.18	8.6
		c_u	G_{max}	1	0.11	24.4

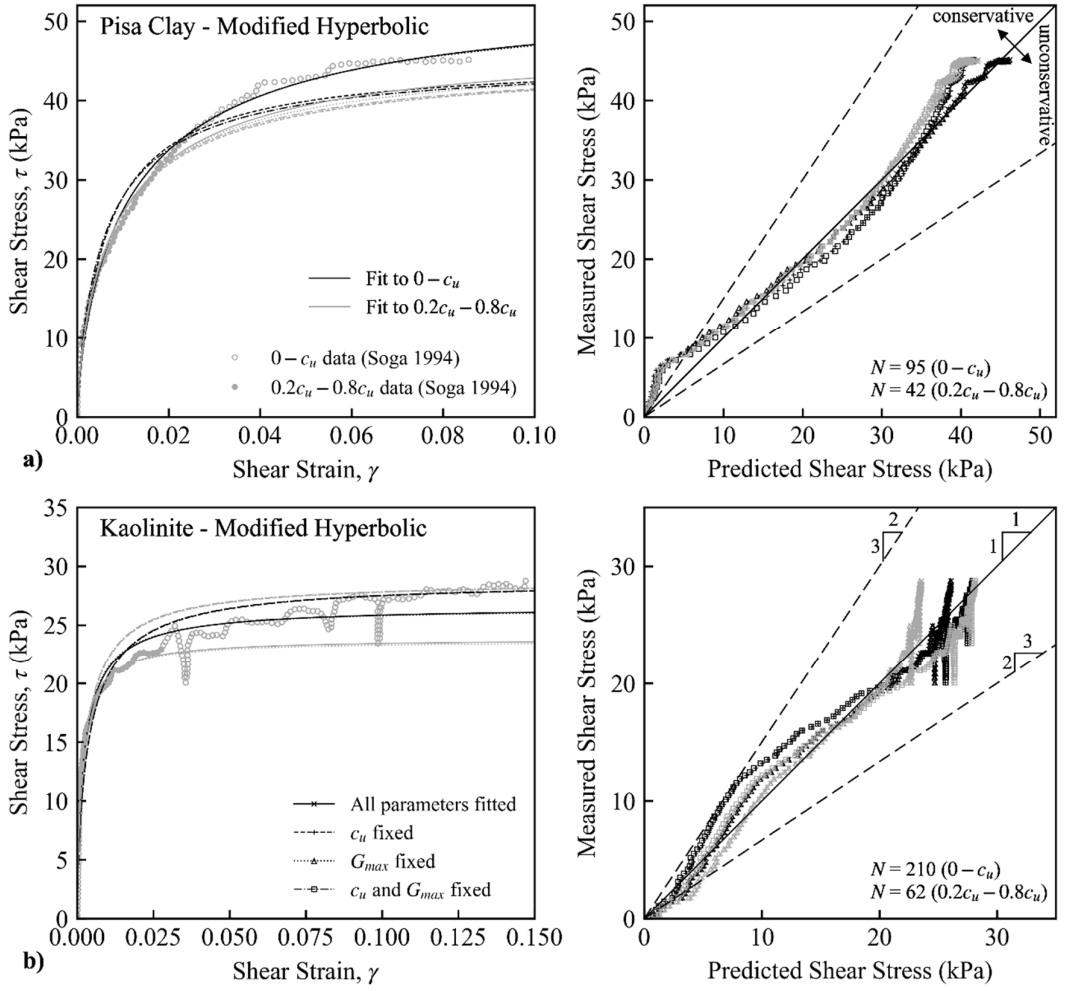

Figure S7: Fitting of the modified hyperbolic model to triaxial data in a) Pisa clay and b) kaolinite. Percentages in parentheses indicate the error bounds. ± 50% prediction bounds are provided for comparison. *N* denotes the number of data points considered in each range. (Data from Soga 1994.)

Table S8: Parameters from the fitting of the exponential model and the respective error bounds. c_u and G_{max} are interpreted values from Soga (1994).

Soil	Range	Parameters			Errors bounds for 95% of data (%)
		τ_{max} (kPa)	G_i (kPa)	R_f	
Pisa	$0 - c_u$	c_u	3,880	1.05	821
		c_u	3,580	1	898
		c_u	G_{max}	1.31	110
		c_u	G_{max}	1	151
	$0.2c_u - 0.8c_u$	c_u	5,810	1.39	63
		c_u	3,740	1	138
		c_u	G_{max}	1.84	77
		c_u	G_{max}	1	152
Kaolinite	$0 - c_u$	c_u	10,630	1.16	43
		c_u	7,440	1	96
		c_u	G_{max}	1.26	263
		c_u	G_{max}	1	293
	$0.2c_u - 0.8c_u$	c_u	14,150	1.40	16.8
		c_u	7,240	1	103
		c_u	G_{max}	1.77	113
		c_u	G_{max}	1	209

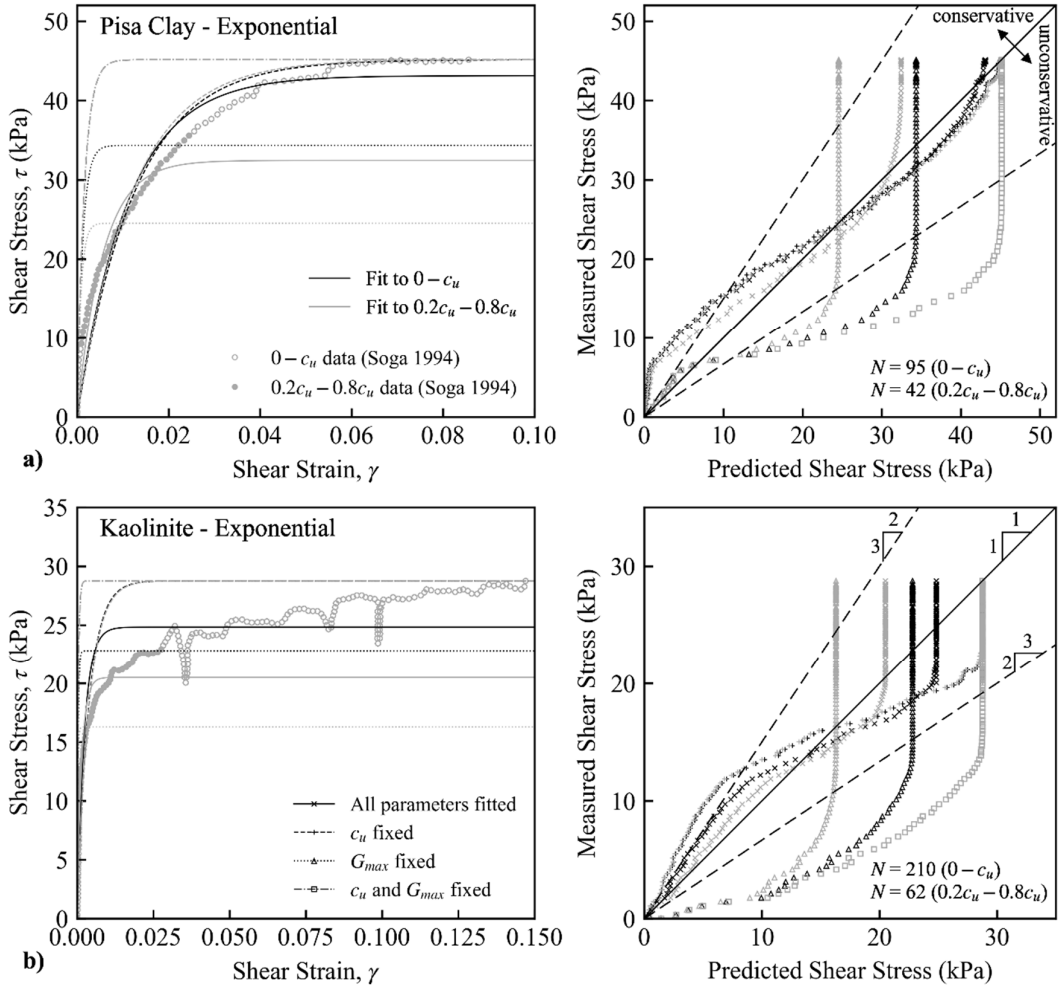

Figure S8: Fitting of the exponential model to triaxial data in a) Pisa clay and b) kaolinite. Percentages in parentheses indicate the error bounds. ± 50% prediction bounds are provided for comparison. *N* denotes the number of data points considered in each range. (Data from Soga 1994.)

References

Leung, Y.F., Soga, K., Lehane, M. and Klar, A. 2010. "Role of linear elasticity in pile group analysis and load test interpretation". *Journal of Geotechnical Engineering, ASCE*, 136 (12), 1686-1694.

Soga, K. 1994. "Mechanical behaviour and constitutive modelling of natural structured soils." Ph.D. thesis, University of California at Berkeley, Berkeley, CA.

Vardanega, P.J. and Bolton, M.D. 2011. "Strength mobilization in clays and silts." *Canadian Geotechnical Journal*, 48 (10), 1485-1503, Corrigendum 48 (5), 631.